Indian Journal of Pure & Applied Physics
Vol. 62, August 2024, pp. 631-637
DOI: 10.56042/ijpap.v62i8.10737

XRD, Electrical, Mechanical, Second and Third-Order NLO Studies of L-Leucinium Perchlorate Crystal

M Arul Tresa[a,*], B Helina[b] & S C Vella Durai[c]

[a]Department of Physics, St. Xavier's College (Autonomous), Palayamkottai, Tirunelveli, Tamilnadu 627 002, India

[b]PG and Research Department of Physics, Sri Paramakalyani College, Alwarkurichi, Tenkasi, Tamilnadu 627 412, India
(Affilated to Manonmaniam Sundaranar University Tirunelveli, 627 012, Tamil Nadu India)

Received 27 April 2024; accepted 9 June 2024

L-Leucine and Perchloric Acid were combined in a 1:1 molar ratio to synthesize L-Leucinium Perchlorate (LLPC) salt, which was subsequently grown into single crystals using a solution method and slow evaporation process. Characterization of the LLPC crystal involved techniques including single crystal X-ray diffraction (XRD), mechanical analysis, dielectric studies, Second Harmonic Generation (SHG) study, Z-scan study, and LDT study. SHG efficiency of the sample, was found to exceed that of potassium dihydrogen orthophosphate (KDP). Mechanical properties such as hardness, yield strength, work hardening coefficient, and stiffness constant were determined for the crystal. XRD analysis confirmed monoclinic crystallization of the LLPC crystal. The findings from numerous investigations were examined and discussed in this paper.

Keywords: NLO; Amino acid complex; Solution growth; Single crystal; Characterization; XRD; NLO; Vicker's hardness; LDT; Z-scan

1 Introduction

There are two types of optics: nonlinear and linear. When a material is exposed to extremely strong laser light, nonlinear optical (NLO) phenomena take place. In terms of technology, this field of study has grown in importance since the invention of the first laser in 1960. NLO materials are essential in the quickly evolving disciplines of photonics, opto-electronics, laser technology *etc*[1-3]. NLO materials are categorized into three primary groups: semiorganic, inorganic, and organic. Among these, organic NLO materials exhibit superior optical susceptibilities, intrinsic ultra-fast response times, and higher laser damage thresholds compared to inorganic NLO crystals[4,5]. Leucine is a vital amino acid that is required for the synthesis of protein and can only be found in diets containing foods like meat, milk, soy products, and beans. Both a beta-amino (NH_3^+) and a beta-carboxylic acid (COO^-) group are present in the beta-amino acid L-leucine[6,7]. An essential component that can be combined with other substances and amino acids to create a variety of NLO crystals is perchloric acid[8–10]. Crystals of L-leucinium oxalate were produced by Anbuchezhiyan *et al.* and reported in multiple studies[11]. Adhikari *et al.* and Subramanian have synthesized and studied L-leucine hyrobromide crystals[12,13]. Some L-leucine-based NLO crystals have been reported in the literature, and L-leucine has apparently been used in supramolecular research as well as crystal engineering[14–17]. Baskaran *et al.* have reported some studies of L-leucinium perchlorate in the literature[18]. In this study, L-leucinium perchlorate, a semiorganic NLO crystal, has been cultivated and examined.

2 Synthesis and crystal growth

L-leucine and perchloric acid were obtained from Merck India, and a 1:1 molar ratio of the reactants was used to create L-leucinium perchlorate. Using stirrer, these ingredients were combined in a borosil beaker and swirled for approximately four hours to create the saturated solution. The reaction temperature wass maintained at 50 ^oC during the stirring. Following the stirring process, the mixture was allowed to reach room temperature (30 ^oC) and then filtered using filter paper to eliminate any remaining suspended particles. L-Leucine and Perchloric acid undergo a chemical reaction to produce L-Leucinium Perchlorate. In a growing jar with a perforated polythene paper cover, the filtered saturated solution was added. After roughly six days, the saturated solution became a supersaturated solution due to sluggish evaporation, at which point tiny crystals

*Corresponding author: (E-mail: tresapaul.kk@gmail.com)

began to form at the growth vessel's bottom. After a growth period of around 40 days, the seed crystals have developed into large crystals upon continued gradual evaporation of the solution. Fig. 1 displays a shot of an LLPC crystal of high quality.

3. Results and Discussion

3.1. XRD study

Bragg's law, expressed by the equation $2d \sin\theta = n\lambda$, serves as the cornerstone of X-ray diffraction (XRD) and is crucial for determining the crystal structure of a crystalline sample. This equation involves parameters such as the wavelength of the X-rays (λ), the diffraction order (n), Bragg's angle (θ), and the interplanar spacing (d)[19]. Single crystal XRD is utilized for samples like LLPC. The lattice parameters of the LLPC crystal were established using a Bruker 4SMART KAPPA APEX II CCD single-crystal X-ray diffractometer with a wavelength (λ) of 0.71073 Å. The unit cell parameters of the LLPC crystal are as follows: a = 5.678(2) Å, b = 8.764 (1) Å, c = 10.711(3) Å, and $\alpha = 90^o$, $\beta = 97.25$ (4), $\gamma = 90^o$, and V = 528.74(2) $Å^3$. Analysis confirms that the LLPC crystal possesses a monoclinic crystal structure. The obtained results for LLPC crystal in this work are observed to be in good agreement with the reported literature[18]

3.2. Mechanical characterization

One of the crucial mechanical characteristics is hardness, which can be used to gauge a material's strength and plastic characteristics. The most common and straightforward static indentation test for determining hardness is the Vickers microhardness test[20]. After the indenter is removed, the permanent impression is kept in the specimen and can be in the shape of a ball, diamond cone, or diamond pyramid. Using a diamond pyramidal indenter, the specimen's surface is micro-indented using this technique. The Vickers microhardness number is determined by the formula $H_v = 1.8544\ P / d^2$, where P represents the applied load and d is the average diagonal length of the indentation. Hardness values are determined by the size of the imprint left on the surface after the removal of a loaded indenter[21]. In this investigation, the thoroughly polished LLPC crystal was positioned on the platform of a Vickers microhardness tester, and loads of different intensities were applied for a fixed duration of ten seconds. Fig. 2 illustrates the correlation between the hardness number (Hv) and the applied load (P) for the LLPC crystal. The graph demonstrates that hardness escalates as the force increases, suggesting the existence of the reverse indentation size effect.

Meyer's law, expressed as $P = ad^n$, serves to determine the work hardening coefficient (n) applicable to the LLPC crystal. In this equation, both a and n are constants specific to the material. Through

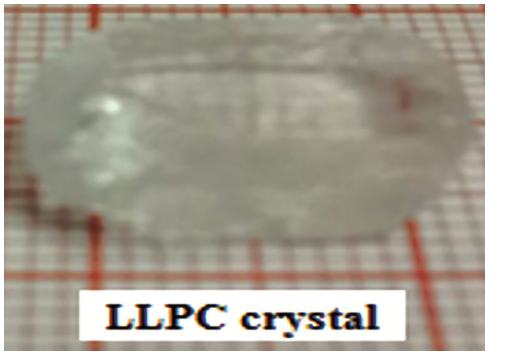

Fig. 1 — A collected crystal of LLPC

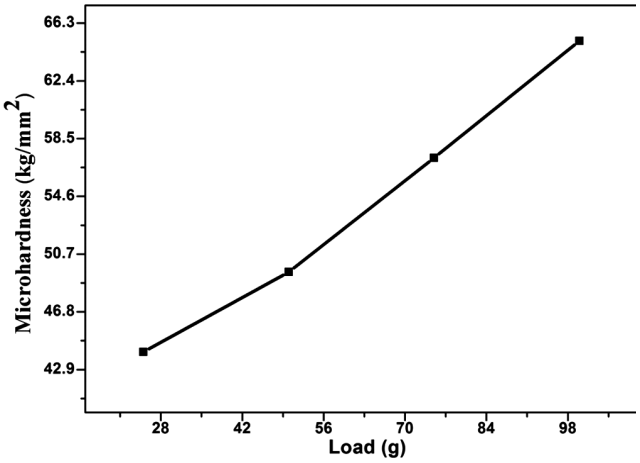

Fig. 2 — Plot of hardness versus applied load for LLPC crystal

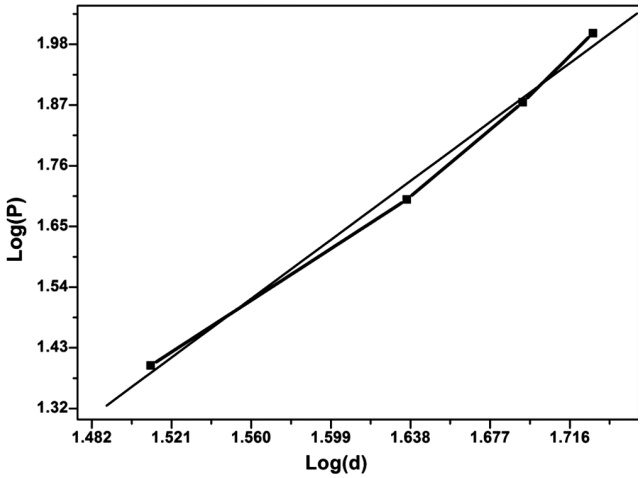

Fig. 3 — Plot of Log (P) versus Log (d) for LLPC crystal

analysis depicted in Fig. 3, the work hardening coefficient (n) for LLPC was calculated to be 2.773. According to Onitsch[22], work hardening coefficient (n) values ranging from 1.0 to 1.6 typically characterize hard materials, while values exceeding 1.6 indicate soft materials. The determination of LLPC as a soft crystalline material is thereby validated. The yield strength (σy) of LLPC crystal can be calculated using the relation σy = (Hv/3) (0.1)n-2, where n represents the work hardening coefficient. Additionally, Wooster's empirical relation C11 = Hv7/4, where Hv denotes the Vickers hardness number, facilitates the calculation of the elastic stiffness constant (C11). Table 1 presents the estimated values for LLPC crystal's hardness, yield strength, and stiffness constant, highlighting their dependence on the applied load[23].

3.3 Second-order NLO study

When a high intensity laser is focused on the crystal, susceptibility becomes field dependent and polarisation becomes independent. The second-order susceptibility is responsible for second-order NLO phenomena such as optical rectification, sum frequency and difference frequency generations, and second harmonic generation (SHG). The LLPC crystal's SHG efficiency was evaluated using the Kurtz-Perry powder method[24,25]. The fundamental wavelength of a 1064 nm Nd:YAG laser was employed in this instance to concentrate on the powdered material, and the input laser energy was 0.7 J/pulse. The KDP reference sample included particles with the same size (150–200 μm) as the LLPC crystalline sample. It was discovered that the KDP and LLPC samples' green laser emission had a wavelength of 532 nm. The laser output energy of the KDP sample and the LLPC sample is 8.8 mJ/pulse and 16.45 mJ/pulse, respectively. Thus, the relative SHG efficiency of LLPC crystalline sample is 1.87 and this value is compared with SHG efficiency of some of the NLO crystals in the Table 2. Since LLPC crystal has high SHG efficiency, it can be used efficiently for NLO applications.

Table 1 — Values of hardness, yield strength and stiffness constant of LLPC crystal

Applied load (grams)	Hardness (kg/mm^2)	Yield strength x 10^6 (pascal)	Stiffness constant (pascal)
25	44.14	2.429	1.295E+15
50	49.52	2.727	1.585E+15
75	57.23	3.151	2.042E+15
100	65.17	3.586	2.561E+15

3.4 Determination of electronic polarizability and other parameters

Various forms of polarizability exist, encompassing electronic, ionic, dipolar, and space charge polarizability. Electronic polarizability describes the inclination of a charge distribution, like electrons or atoms, to alter its typical shape when an electric field is applied to a sample comprising molecules or atoms. The electronic polarizability, along with solid-state parameters such as the Penn gap, Fermi energy, and valence electron plasma energy, can theoretically be quantified. The valence electron plasma energy is calculated by equation[26]

$$E_v = 28.8\,[(Z' \times \rho) / M]^{1/2}\, q \quad \ldots (1)$$

Where M represents the molecular weight of L-leucinium perchlorate (LLPC), Z' denotes the number of valence electrons of LLPC, and signifies the crystal's density. The formula Ep = Ev (ε'- 1)-1/2 can be utilized for computing the Penn gap energy, where ε' represents the dielectric permittivity, also referred to as the dielectric constant, at 1 MHz. The Fermi energy, which can be theoretically calculated using the formula EF = 0.2948 x Ev4/3, represents the kinetic energy of the particles at their highest occupied state. Table 3 presents the calculated plasma energy, Penn gap energy, and Fermi energy of the LLPC crystal. Through Penn gap analysis, the electronic polarizability of the LLPC crystal can be determined using by Eq. 2:

$$\alpha = [(E_v^2\, S) / (E_v\, S + 3E_p^2)] \times (M/\rho) \times 0.396 \times 10^{-24} \quad \ldots(2)$$

where $S = 1 - (E_p/4E_F) + 1/3\,(E_p/4E_F)^2$. In this case, S is a constant for a certain substance. The electronic

Table 2 — Relative SHG efficiency of some the NLO crystals

S.No.	Crystal name	Relative SHG efficiency (Reference sample: KDP)	Reference
1.	L-leucinium oxalate	0.7	11
2.	L-histidine	3	24
3.	hydrochloride	2.4	25
4.	monohydrate crystal	1.87	Current study
	Amaranth and EDTA co-doped KDP crystals		
	L-lecinium perchlorate		

Table 3 — Plasma energy, Penn gap energy and Fermi energy of LLPC crystal

Solid state parameters	Values
Plasma energy	21.034 eV
Penn gap energy	10.331 eV
Fermi energy	7.273 eV

polarizability of the LLPC crystal is determined by the Penn analysis to be 4.175 x 10^{-23} cm^3. The value of the sample's electronic polarizability can also be determined using the Clausius-Mossotti relation as given Eq. 3[27-29].

$$\alpha = (3M/4\pi N\rho)\,[(\varepsilon'-1)/(\varepsilon'+2)] \quad \ldots(3)$$

where N is the Avogadro's number and 4.142 x 10^{-23} cm^3 is the calculated electronic polarizability value.

3.5 LDT value of the crystal

Experiments assessing the laser damage threshold (LDT) of the produced LLPC crystal were carried out employing a Nd:YAG laser featuring an 18 ns pulse width and a wavelength of 1064 nm. A coherent energy/power meter (Model No. EPM 200) was employed to gauge the energy of the laser beam. The equation P = E/τπr2, where E represents the energy, τ stands for the pulse width, and r denotes the spot radius, was utilized to determine the LDT value[30]. High power laser light interacts with the crystal in a way that causes laser damage. Several processes, including optical, thermal, chemical, and physical ones, are involved. For the LLPC crystal, the computed LDT value is 2.91 GW/cm^2. Given its great value, LLPC crystals can be utilized in the production of laser-related devices. For comparison purpose, LDT values of some of the important NLO crystals are provided in the Table 4.

3.6 Dielectric study

An electrical insulator that can become polarised when an electric field is applied is called a dielectric. Dielectric polarisation results from the electric charges in a dielectric shifting slightly from their usual equilibrium positions in an electric field, as opposed to flowing through the material as they would be in a conductor. The real capacitance of a capacitor filled with a dielectric material is ε_r times higher than that of a capacitor with the same electrodes in vacuum. The ratio of a capacitor's capacitance with that material acting as its dielectric to a similar capacitor with a vacuum acting as its dielectric is known as the dielectric constant. A material's static relative permittivity, also referred to as its dielectric constant, is its relative permittivity at a frequency of zero. Dielectric loss, commonly associated with losses occurring under alternating voltage, quantifies the power dissipation in a dielectric material due to applied voltage. The dielectric loss angle is a crucial parameter for both dielectric materials and insulated sections. When subjected to an alternating field, a phase shift arises between the displacement and the applied field. Thus, it can be said that the dielectric constant is a complicated quantity and it is given equation

$$\varepsilon = \varepsilon' - i\varepsilon'' \quad \ldots(4)$$

and ε"/ε' = tan δ, where tan δ is called the dielectric loss factor[34]. Measurements of capacitance and the dielectric loss factor (tan δ) were carried out using a parallel plate capacitor across temperatures ranging from 30 to 70 °C. An Agilent 4284A LCR meter was employed at frequencies spanning from 100 Hz to 1 MHz. To ensure a conductive surface layer, the contact faces of the crystal were coated with graphite. The accuracy of dielectric parameter measurements was maintained within ± 5%. Figs 4 & 5 illustrate variations in the dielectric constant and dielectric loss of the LLPC crystal concerning frequency. Notably, both parameters decrease with increasing frequency and increase with rising temperature. The observed peaks in dielectric constant at low frequencies are attributed to space charge polarization, while the decline may result from the gradual reduction of various polarization types. Higher dielectric constants at elevated temperatures are typically associated with crystal expansion, electronic and ionic polarizations, and the presence of crystal defects[31-37].

Table 4 — LDT values of some important nonlinear optical (NLO) crystals

S. No.	Sample name	Value of LDT (GW/cm^2)	Reference
1.	Urea	0.35	31
2.	Benzamidazole Crystal	1.71	32
3.	L-Prolinium Tartrate	5.90	33
4.	L-Lecinium Perchlorate	2.91	Present work

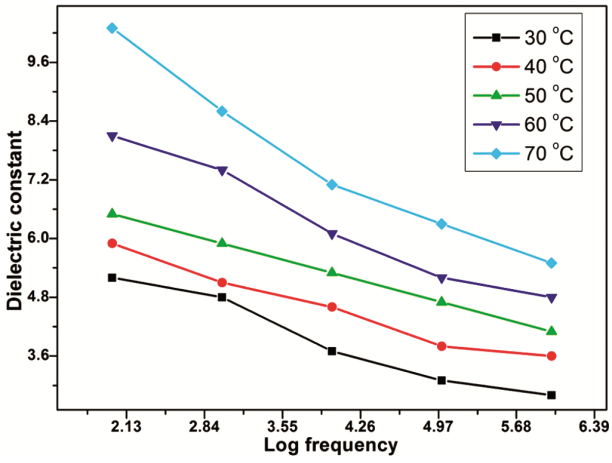

Fig.4 — Frequency dependence of dielectric constant for LLPC crystal at different temperatures

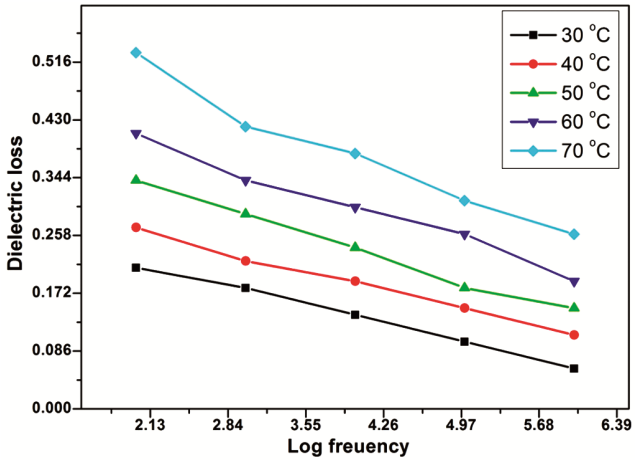

Fig. 5 — Frequency dependence of dielectric loss for LLPC crystal at different temperatures

3.7 Third-order NLO study

To investigate the LLPC crystal using Z-scan, we utilized a He-Ne laser with a wavelength of 632.8 nm. This technique is widely accepted in nonlinear optics for detecting nonlinear changes in absorption and refractive index. Our study focuses on third-order nonlinear optics, with the sample's third-order NLO characteristics—nonlinear absorption coefficient (β), nonlinear susceptibility (χ(3)), and nonlinear refractive index (n2)—being calculated. Furthermore, the Z-scan method allows determining the sign of the nonlinear refractive index. Key steps of the Z-scan involve placing the thin sample along a focused Gaussian laser beam, moving it along the Z-direction into the focal region, and converting phase distortion to amplitude distortion during propagation.

Peak to valley or valley to peak Z-scan curves can be generated by using the closed aperture approach. One feature of self-focusing is the transmittance variation from peak to valley. The difference value in transmission between peak and valley (ΔT_{p-v}) is

$$\Delta T_{p-v} = 0.406\ (1-S)^{0.25} |\ \Delta\Phi| \quad \ldots(5)$$

where S is the linear aperture transmittance and $|\Delta\Phi|$ is the axis phase shift.

$$S = 1 - \exp\left(\frac{-2r_a^2}{\omega_a^2}\right) \quad \ldots(6)$$

where r_a and ω_a are the aperture radius and beam radius respectively.

The following relation is used to compute the third-order nonlinear refractive index, n2:

$$n_2 = \frac{\Delta\Phi\lambda}{2\pi I_o L_{eff}} \quad \ldots(7)$$

The sample's effective thickness (L_{eff}) equals

$$L_{eff} = \frac{[1-\exp(-\alpha L)]}{\propto} \quad \ldots(8)$$

where L and ∝ are the LLPC crystal's thickness and linear absorption coefficient, respectively, and β represents the nonlinear absorption coefficient and it is given by

$$\beta = \frac{2\sqrt{2\Delta T}}{I_O\ L_{eff}} \quad \ldots(9)$$

The nonlinear absorption coefficient doesn't impact the nonlinear refractive index, allowing us to use these relationships to determine third-order responses or the real and imaginary components of the third-order nonlinear optical susceptibility. Therefore, we can find the third-order responses and the real and imaginary parts of the third-order nonlinear optical susceptibility using the following equations:

$$Re\,x^{(3)} = \frac{10^{-4} s_o c^2\ n_o^2\ n_2}{\pi} \quad \ldots(10)$$

$$Im\ x^{(3)} = \frac{10^{-2} s_o\ c^2\ n_o^2\ \lambda\beta}{4\pi^2} \quad \ldots(11)$$

Hence, the absolute value of third order nonlinear optical susceptibility is equal to

$$|x|\ |x| = \sqrt{(Re\ x^{(3)})^2 + (Im\ x^{(3)})^2} \quad \ldots(12)$$

Using the above equations, the third order NLO parameters of the grown LLPC crystal could be estimated[38-42].

The normalised transmittance of an LLPC crystal in both open and closed aperture modes has been measured by adjusting the sample location (Z). Figs 6 & 7 show the LLPC crystal's open aperture and closed aperture curves. The closed aperture curve exhibits a prefocal transmittance max. and a post focal transmittance min. intensity, indicating the LLPC crystal's negative non-linear refractive index. Conversely, the open aperture Z-scan curve illustrates that the transmitted intensity peaks at the focus, confirming the occurrence of saturable absorption within the sample. Calculations yield the nonlinear absorption coefficient (β), third-order nonlinear susceptibility (χ(3)), and nonlinear refractive index (n2) for the LLPC crystal as 3.305 x 10^{-10} m^2/W, 6.351 x 10^{-5} m/W, and 7.493 x 10^{-6}, respectively. Given its negative nonlinear refraction, the LLPC crystal proves valuable in applications such as optical night vision sensor devices, optical switching, and sensor protection[43-45].

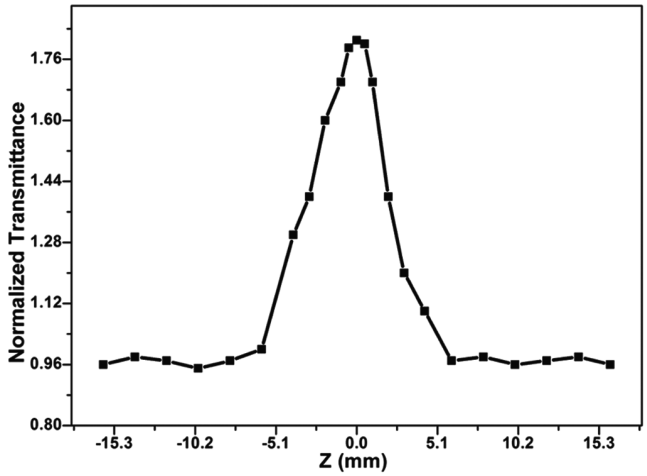

Fig. 6 — Open aperture Z-scan curve for LLPC crystal

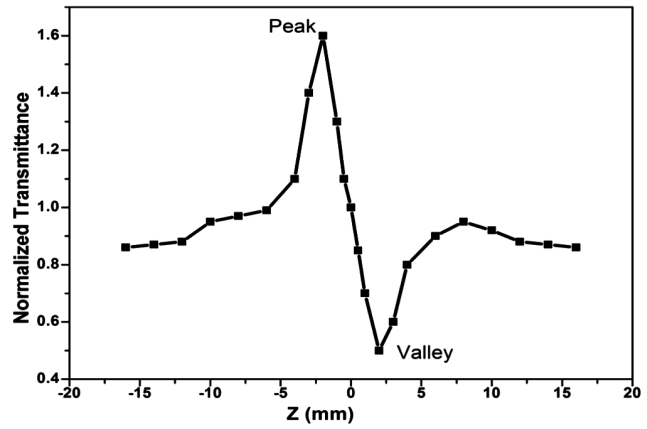

Fig. 7 — Closed aperture Z-scan curve for LLPC crystal

4 Conclusion

LLPC single crystals were cultivated using a solution method with controlled slow evaporation. Analysis via XRD revealed that the resulting crystal adopts a monoclinic crystal system. Notably, the SHG efficiency of the LLPC crystal surpassed that of the KDP crystal by a factor of 1.87. Investigation into the dielectric properties of the sample, including dielectric loss and dielectric constant, was conducted across various frequencies and temperatures. Electronic polarizability of the LLPC crystal was determined to be 4.142 x 10^{-23}cm^3. Furthermore, the projected LDT value for the LLPC crystal stands at 2.91 GW/cm^2. Through Z-scan analysis, the third-order nonlinear optical parameters were ascertained to be 3.305 x 10^{-10} m^2/W, 6.351 x 10^{-5} m/W, and 7.493 x 10^{-6} esu. The LLPC crystal exhibits promise for both second-order and third-order NLO applications, including optical computers, night vision sensor devices, optical switching devices, and second harmonic generators, owing to its superior SHG efficiency, high LDT value, and negative nonlinear refraction.

References

1 Razzetti C, Ardoino M, Zanotti L, Zha M & Paorici C, *Cryst Res Technol*, 37 (2002) 456.
2 Narayan Bhat M & Dharmaprakash S M, *J Cryst Growth*, 236 (2002) 376.
3 Rodrigues J J, Misoguti L, Nunes F D, Mendonca C R & Zilio S C, *Opt Mat*, 22 (2003) 235.
4 Tanusri Pal, Tanusree Kar, Gabriele Bocelli & Lara Rigi, *Cryst Growth Des*, 3 (2003) 13.
5 Natarajan S, Martin Britto S A & Ramachandran E, *Cryst Growth Des*, 6 (2006) 137.
6 Kumari N, Yadav A A, Sankpal S A, Murugavel S, Lakshmanan D & Kant R, *Indian J Pure Appl Phys*, 61 (2023) 798.
7 Aarthy J, Suriya M, Sakthi Murugesan K & Milton Boaz B, *Indian J Pure Appl Phys*, 60 (2022) 763.
8 Janczak J & Perpetuo G J, *Acta Cryst*, C63 (2007) 117.
9 Marchewka M K & Drozd M, *Cent Eur J Chem*, 11 (2013) 1264.
10 Mallik T & Kar T, *J Cryst Growth*, 274 (2005) 251.
11 Anbuchezhiyan M, Ponnusamy S & Muthamizhchelvan C, *Optoelectron Adv Mater – Rapid Commun*, 3 (2009) 1161.
12 Adhikari S & Kar T, *Mater Res Bull*, 48 (2013) 1612.
13 Subramanian E, *Acta Cryst,* 22 (1967) 910.
14 Hemalatha A, Arulmani S, Sanjay P, Deepa K, Madhavan J & Senthil S, *IOP Conf Ser: Mater Sci Eng*, 360 (2018) 012044.
15 Senthil R, Vijayaraghavan G, Ismail Fathima M, Beer Mohamed S & Ayeshamariam A, *Asian J Chem,* 34 (2022) 931.
16 Jagadeesh M R, Suresh Kumar H M & Ananda Kumari R, *Mater Sci -Pol*, 33 (2015) 529.
17 Ansari A A, Prakash J, Nidhi, Aafreen, Chauhan S & Singh G, *Indian J Pure Appl Phys*, 62 (2024) 109.
18 Baskaran P, Vimalan M, Anandan P, Bakiyaraj G, Krubavathi K & Selvaraj K, *J Taibah Uni Sci*, 11 (2017) 11.
19 Cullity B D, Elements of X-ray Diffraction, Addison-Wesley publishing company (1977).
20 Lawn B R & Puller D R, *J Mater Sci*, 9 (1975) 2016.
21 Mott B W, Micro Indentation Hardness Testing, Butterworths, London, 1956.
22 Onitsch E M, *Mikroskopie*, 95 (1988) 12.
23 Balakrishnan T & Ramamurthi K, *Mater Lett*, 62 (2008) 65.
24 Kurtz S K & Perry T T, *J Appl Phys*, 39 (1968) 3798.
25 Anandan P, Jayavel R, Saravanan T, Parthipan G, Vedhi C & Mohan Kumar R, *Opt Mater*, 34 (2012) 1225.
26 Phan V T, Do T T P, Nguyen D T, Nguyen K D, Vo T T N, Le A T Q & Huynh D T, *Opt Quant Electron*, 53 (2021) 1.
27 Karuppasamy P, Sivasubramani V, Senthil Pandian M & Ramasamy P, *RSC Adv*, 6 (2016) 109105.
28 Penn D R, *Phys Rev*, 128 (1962) 2093.
29 Ravindra N M & Srivastava V K, *J Infrared Phys*, 20 (1980) 67.
30 Reddy R R, Nazeer A Y & Ravi K M, *J Phys Chem Solids*, 56 (1995) 825.
31 Vivek P & Murugakoothan P, *Optik*, 124 (2013) 3510.

32 Bhar G C, Chaudhary A K & Kumbhakar P, *Appl Surf Sci*, 161 (2000) 155.
33 Vijayan N, Bhagavannarayana G, Kanagasekaran T, Babu R R, Gopalakrishnan R & Ramasamy P, *Cryst Res Technol*, 41 (2006) 784.
34 Martin Britto Dhas S A & Natarajan S, *Cryst Res Technol*, 42 (2007) 471.
35 Van Hippel, Dielectric Theory of Solids, MIT Press, U.S.A (1954).
36 Selvarajan P, Das B N, Gon H B & Rao K V, *J Mater Sci*, 29 (1994) 4061.
37 Rao K V & Samakula A, *J Appl Phys*, 36 (1995) 2031.
38 Lucia Rose A S J, Selvarajan P & Perumal S, *Spectrochim Acta,* 481 (2011) 270.
39 Sheik B, et.al *IEEE J Quant Electron*, 26 (1990) 760.
40 Shanthi A, Krishnan C & Selvarajan P, *Spectrochemica Acta Part A: Molecular and Biomolecular Spectroscopy*, 122 (2014) 521.
41 Bahae M S, Said A A & Van Stryland E W, *Optics -Opt Lett*, 14 (1989) 955.
42 Peramaiyan G, Pandi P, Jayaramakrishnan V, Subhasis Das & Mohan K R, *Optical Mater,* 35 (2012) 307.
43 Karuppasamy P, Senthil P M & Ramasamy P, *J Cryst Growth*, 473 (2017) 39.
44 Azhar S M, Rabbanib G, Shirsat M D, Hussaini S S, Baig M I, Ghramh H A & Mohd Anis, *Optik*, 165 (2018) 259.
45 Said A A, Xia T, Hagan D J, Van Stryland E W & Sheik-Bahae M, *J Opt Soc Am B: Opt Phys*, 14 (1997) 824.